

Anisotropy of the conduction band of InSb: Orbital and spin properties

W. Zawadzki,* I. T. Yoon, C. L. Littler, and X. N. Song

Department of Physics, University of North Texas, Denton, Texas 76203

P. Pfeffer

Institute of Physics, Polish Academy of Sciences, 02-668 Warsaw, Poland

(Received 27 May 1992)

The anisotropy of the conduction band of InSb has been investigated experimentally and theoretically. Spin-conserving and spin-flip harmonics of cyclotron resonance, as well as phonon-assisted harmonics of cyclotron resonance, have been observed for the magnetic-field orientations $\mathbf{B} \parallel [001]$ and $\mathbf{B} \parallel [111]$. In order to measure precisely small differences in the resonant field positions of the magneto-optical spectra, the photoconductive signals have been detected simultaneously from two differently oriented samples excited by a single beam of CO₂ laser radiation. The results permit us to separate the anisotropy of the effective mass from that of the spin g value. The data have been successfully described by the five-level $\mathbf{k} \cdot \mathbf{p}$ model, which accounts for the nonparabolicity and nonsphericity of the Γ_6^c conduction band. From fitting the experimental anisotropy we have determined the momentum matrix element between the higher conduction (Γ_6^c, Γ_7^c) and valence (Γ_8^v, Γ_9^v) levels: $E_Q = 13.99$ eV. It has been found that the anisotropy of the g value is considerably larger than that of the effective mass. This feature results automatically from the theory, although within the five-level model only the single matrix element Q is responsible for the band's anisotropy. In addition to the free-electron transitions, we have also observed the transitions of electrons bound to magnetodonors. These excitations have also been successfully described by a combination of the five-level $\mathbf{k} \cdot \mathbf{p}$ theory and the magnetodonor theory. It has been found that the orbital and spin anisotropies of the bound electron energies are the same as those of the free-electron energies.

I. INTRODUCTION

InSb has been for many years considered to be a model narrow-gap semiconductor and its band structure has been investigated both experimentally and theoretically by numerous authors. It was recognized early by Kane¹ that, as a result of the small energy gap, the conduction band of this material has a nonparabolic energy-wave-vector relation. Kane's theoretical results were confirmed by many diverse experiments (cf. Zawadzki, Ref. 2). On the other hand, there exist few works concerned with the conduction band's anisotropy. Antcliffe and Stradling³ and Seiler⁴ used the Shubnikov-deHaas effect to show that the Fermi surface is slightly anisotropic, while McCombe⁵ and Chen, Dobrowolska, and Furdyna⁶ studied the anisotropy of the Lande g factor using combined and spin resonance, respectively.

Magneto-optical data, providing precise information on the band structure, are demanding tests on the validity of theoretical models. The first nonparabolic description of the conduction band of InSb in the presence of a magnetic field was given by Bowers and Yafet.⁷ Their three level ($3L$) model took into account the $\mathbf{k} \cdot \mathbf{p}$ interaction between the conduction Γ_6^c level, the valence Γ_8^v level and the Γ_7^v level split off from the Γ_8^v level by the spin-orbit energy Δ . This approach is quite good for describing the conduction band and the split-off valence band. The resulting energy bands are spherical, with the effective masses and g factors depending on energy (cf. Zawadzki, Ref. 8). The $3L$ model gives a cubic equation for the orbital and spin energies. If one is interested in electron en-

ergies which are not too high, the cubic equation can be approximated well by a quadratic equation, which is solved in terms of square roots.

A phenomenological modification of the square-root approximation, due to Johnson and Dickey,⁹ has often been used for the interpretation of experimental data. The modification amounts to taking into the square-root expression for the energies the measured band-edge values of the effective mass m_0^* and the effective g factor g_0^* . This approach, although not rigorous theoretically, effectively includes the influence of distant bands on the conduction band in question.

The $3L$ model has two shortcomings. First, it does not describe the heavy-hole band, whose curvature results from the $\mathbf{k} \cdot \mathbf{p}$ interaction with distant bands. Second, it fails to account for the Luttinger effects¹⁰ (sometimes called "quantum" effects), i.e., the irregular spacing of the light- and heavy-hole Landau levels for low quantum numbers n . The Luttinger effects are due to the degeneracy of the Γ_8 bands at $\mathbf{k}=0$, which "mixes" the light- and heavy-hole states.

The above deficiencies were removed in the model proposed by Pidgeon and Brown¹¹ (PB), which supplements the $3L$ model with the $\mathbf{k} \cdot \mathbf{p}$ interactions with distant bands up to k^2 terms. The bands resulting from the PB description are both nonparabolic and nonspherical. In the spherical approximation for the conduction band the PB model is almost equivalent to the Bowers and Yafet description (cf. Zawadzki, Ref. 12). In the PB scheme, some nonspherical terms were neglected in order to factorize the initial set of eight differential equations into

two sets of four equations, soluble in terms of harmonic-oscillator functions. An inclusion of the full band's anisotropy does not admit such solutions. A complete version of the PB approach for the $\mathbf{B}||[001]$ crystal direction was given by Grisar *et al.*,¹³ and for $\mathbf{B}||[001]$, $\mathbf{B}||[011]$, and $\mathbf{B}||[111]$ by Weiler, Aggarwal, and Lax.¹⁴ The PB model has been used to describe numerous intraband and interband magneto-optical experiments on InSb. Fits to various data resulted in somewhat different band parameters, as reviewed by Littler *et al.*¹⁵

Recently, Pfeffer and Zawadzki¹⁶ developed a five-level ($5L$) model, in which the $\mathbf{k}\cdot\mathbf{p}$ interaction between the Γ_7^c , Γ_8^c , Γ_6^c , Γ_8^v , and Γ_7^v levels is explicitly taken into account. This approach, as compared to the $3L$ model, includes the influence of two higher conduction levels. In the $5L$ model the band's anisotropy is described by a single matrix element of momentum Q , which couples the valence levels to the higher conduction levels. Although Q does not affect the conduction-band edge Γ_6^c , it results in an anisotropic conduction band, since away from the band edges all bands are coupled. The $5L$ model has been used to describe the medium gap materials GaAs and InP, for which the $3L$ scheme is not adequate.¹⁷⁻¹⁹

A different approach to the description of nonparabolic and nonspherical energy bands has been proposed by Ogg²⁰ (cf. also Ref. 21). It is based on an expansion of the $\epsilon(\mathbf{k})$ relation in powers of k , up to k^4 terms. However, such an expansion does not suffice for narrow gap materials such as InSb.

The purpose of this work is to study the anisotropic orbital and spin properties of conduction electrons in InSb.²² This is done by means of intraband magneto-optical experiments, in which the magnetic field is oriented along either the $[001]$ or $[111]$ crystal axes. In the theoretical description we use the $5L$ model for reasons of convenience, since the scheme has already been worked out in detail in Ref. 16. However, we believe that complete solutions based on the matrices of Weiler, Aggarwal, and Lax,¹⁴ (i.e., taking into account the full band's anisotropy according to the Evtuhov²³ procedure) should give for InSb similar results.

II. THEORETICAL FRAMEWORK

Since the theory of the $5L$ model has been presented in detail elsewhere (cf. Ref. 16), we will summarize here only the main points of this treatment. The initial eigenvalue problem for one electron in a periodic potential and an external magnetic field reads

$$\left[\frac{1}{2m_0} \mathbf{p}^2 + V_0(r) + \frac{\hbar}{4m_0^2 c^2} (\boldsymbol{\sigma} \times \nabla V_0) \cdot \mathbf{p} + \mu_B \mathbf{B} \cdot \boldsymbol{\sigma} \right] \Psi = E \Psi, \quad (1)$$

where $\mathbf{P} = \mathbf{p} + e \mathbf{A}$ is the kinetic momentum, \mathbf{A} is the vector potential of the magnetic field \mathbf{B} , and the Pauli term is written in the standard notation. We seek solutions in the form

$$\Psi = \sum_l f_l(\mathbf{r}) u_l(\mathbf{r}), \quad (2)$$

in which $u_l(\mathbf{r})$ are the Luttinger-Kohn periodic functions and $f_l(\mathbf{r})$ are the envelope functions, slowly varying with the unit cell. The summation is over all energy bands. Inserting (2) into (1), multiplying on the left by $(1/\Omega) u_l^*$, and integrating over the unit cell, one obtains

$$\sum_l \left[\left(\frac{1}{2m_0} P^2 + E_l - E \right) \delta_{l'l} + \frac{1}{m_0} \mathbf{p}_{l'l} \cdot \mathbf{P} + \mu_B \mathbf{B} \cdot \boldsymbol{\sigma}_{l'l} + H_{ll}^{s.o.} \right] f_l = 0, \quad (3)$$

$$l' = 0, 1, 2, \dots$$

where $\mathbf{p}_{l'l}$ and $\boldsymbol{\sigma}_{l'l}$ are the interband matrix elements of the momentum and the spin operators, respectively. Equation (3) represents a set of coupled differential equations for the envelope functions f_l .

The $5L$ model is defined by specifying the Luttinger-Kohn band-edge states for the five levels in question: Γ_7^c , Γ_8^c , Γ_6^c , Γ_8^v , and Γ_7^v . Within this model there exist three different matrix elements of momentum,

$$P_0 = -\frac{i\hbar}{m_0\Omega} \langle S | p_x | X \rangle, \quad P_1 = -\frac{i\hbar}{m_0\Omega} \langle S | p_x | X' \rangle, \quad (4)$$

$$Q = -\frac{i\hbar}{m_0\Omega} \langle X | p_y | Z' \rangle = \frac{i\hbar}{m_0\Omega} \langle X' | p_y | Z' \rangle,$$

and three spin-orbit energies,

$$\Delta_0 = -\frac{3i\hbar}{4m_0^2 c^2} \langle X | [\nabla V_0, \mathbf{p}]_y | Z \rangle,$$

$$\Delta_1 = -\frac{3i\hbar}{4m_0^2 c^2} \langle X' | [\nabla V_0, \mathbf{p}]_y | Z' \rangle, \quad (5)$$

$$\bar{\Delta} = -\frac{3i\hbar}{4m_0^2 c^2} \langle X | [\nabla V_0, \mathbf{p}]_y | Z' \rangle.$$

In the above definitions S denotes the symmetry of the Γ_6^c level, X and Z the symmetries of the Γ_8^v and the Γ_7^v valence levels, and X' and Z' the symmetries of the Γ_8^c and Γ_7^c conduction levels. The values of Δ_0 and Δ_1 are measured experimentally (cf. Fig. 1), the value of $\bar{\Delta}$ is calculated by pseudopotential methods,²⁴ and the values of P_0 , P_1 , and Q are treated as adjustable parameters. The $5L$ model involves altogether 14 Luttinger-Kohn states, so that the set (3) represents 14 differential equations. If the matrix element Q is assumed to vanish, the resulting energy bands are spherical,²⁵ the problem in the presence of a magnetic field has cylindrical symmetry. In this case, the 14 envelope functions are simple harmonic-oscillator functions, and the energies do not depend on the orientation of the magnetic field with respect to the crystal axes.

In the real case of $Q \neq 0$, the energy bands are not spherical. Now one has to specify the orientation of the magnetic field by properly choosing the gauge of the vector potential \mathbf{A} . Since the situation in a magnetic field differs only slightly from having cylindrical symmetry, one looks for envelope functions f_l in the form of sums of harmonic-oscillator functions.²³ The differential eigen-

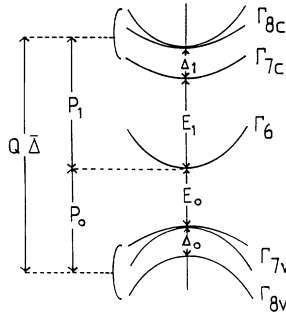


FIG. 1. Five-level model of the band structure near the Γ point of the Brillouin zone. The interband matrix elements of momentum and of the spin-orbit interaction are indicated.

value problem is then transformed into a diagonalization of an infinite number matrix. The latter is truncated in order to obtain a good approximation for the energies in question and diagonalized numerically.

It has been observed by Weisbuch and Hermann²⁶ that the experimental values of the effective mass m_0^* and the effective g factor g_0^* in III-V compounds cannot be described theoretically with the help of P_0 and P_1 alone (the conduction-band-edge values are not affected by Q). Consequently, one needs to account for some influence of distant bands. This is done by adding small contributions C and C' to the band-edge values m_0^* and g_0^* , respectively. Thus, all in all, the 5L model in our version includes five adjustable parameters, of which only Q is responsible for the band's anisotropy.

III. EXPERIMENTAL PROCEDURE

The experiments were performed on high-purity samples of n -type InSb with a carrier concentration of $9 \times 10^{13} \text{ cm}^{-3}$ and an electron mobility of $7 \times 10^5 \text{ cm}^2/\text{V-sec}$ at 77 K. The samples were rectangular slabs, whose surfaces were lapped using alumina grit and then chemically etched using a 2% bromine-methanol solution. Electrical contacts were made to the samples using pure indium. The output of a grating-tunable cw CO_2 laser was mechanically chopped into 20- μ -sec-wide pulses at a low duty cycle to prevent lattice-heating effects. The laser radiation was focused onto the samples situated in a superconducting magnet housed in a low-temperature cryostat. The system is capable of supplying dc magnetic fields up to 12 T and temperatures as low as 1.8 K. For all measurements the Faraday configuration was used. The magnet also contains modulation coils which can be used to superimpose a small (up to ± 0.1 T) ac magnetic field on the larger dc field. Lock-in amplifier techniques were employed to obtain derivativelike data.²⁷ Photoconductive measurements were used to detect the small changes in absorption resulting from the cyclotron-resonance-type transitions under investigation. All spectra represent the second derivative of the photoconductive response versus magnetic field.

In the case of an anisotropic energy band, the cyclotron frequencies for different magnetic-field orientations

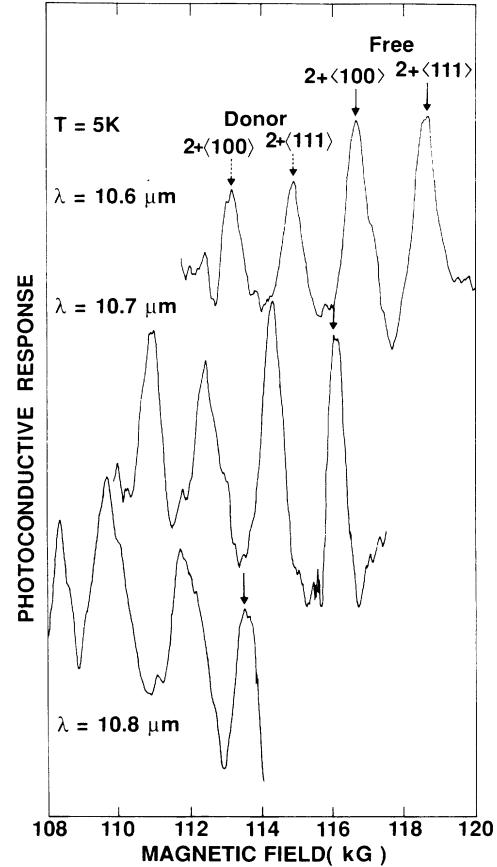


FIG. 2. Second harmonics of cyclotron resonance of free and magnetodonor electrons for different laser wavelengths, as observed simultaneously on two differently oriented InSb samples.

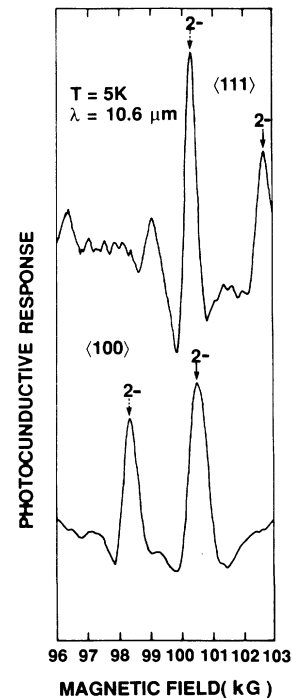


FIG. 3. Second harmonics of cyclotron resonance plus spin flip for free and magnetodonor electrons, as observed on two differently oriented InSb samples.

with respect to the crystal axes are different. However, the measurement of slightly different cyclotron frequencies offers serious technical problems. If one took a separate magnetic-field sweep for a given orientation of \mathbf{B} , the magnet would have to be calibrated very precisely to assure that the slightly different resonant \mathbf{B} values are actually related to the band anisotropy. We have circumvented the problem of precise magnetic-field calibration by detecting the resonance signals simultaneously from two differently oriented samples. In the arrangement we used, the peaks from two differently oriented samples appear in the same field sweep. Consequently, the resonant field differences can be measured precisely, even if the absolute field positions are not known to the same accuracy. Figure 2 shows the free-electron and magnetodonor spin-conserving second harmonics of cyclotron resonance for different laser wavelengths, while Fig. 3 shows the second harmonics of combined resonance (cyclotron resonance plus spin flip) for the differently oriented samples. The mechanism for such transitions has been discussed in Ref. 28.

IV. RESULTS AND DISCUSSION

In this section we discuss the data on the band anisotropy and compare them with the results of the $5L$ $\mathbf{k}\cdot\mathbf{p}$ model. We first consider the free-electron results and then the donor-bound electron results.

A. Conduction electrons

All observed magneto-optical transitions of free electrons originate from the lowest spin-up 0^+ Landau level. The available CO_2 laser frequencies and magnetic fields did not allow us to observe the fundamental cyclotron resonance (CR) transition $0^+ \rightarrow 1^+$. Instead, we observed the transitions $0^+ \rightarrow 2^+$ (second harmonic of CR), $0^+ \rightarrow 2^-$ (second harmonic of CR plus spin flip), $0^+ \rightarrow 2'^+$ (second harmonic of CR assisted by an optic-phonon emission), and $0^+ \rightarrow 3^+$ (third harmonic of CR). For the field orientation $\mathbf{B} \parallel [111]$ and the light polarization $\mathbf{E} \perp \mathbf{B}$ the $2\omega_c$ ($0^+ \rightarrow 2^+$) and the $2\omega_c + \omega_s$ ($0^+ \rightarrow 2^-$) transitions are allowed due to the inversion asymmetry of InSb.¹⁴ The observed transition $3\omega_c$ ($0^+ \rightarrow 3^+$), however, is not allowed for this field orientation. The same difficulty is encountered for the transition $2\omega_c$ for $\mathbf{B} \parallel [001]$, which is not allowed (cf. Favrot, Aggarwal, and Lax, Ref. 29). The current (not confirmed) interpretation is that such forbidden transitions become allowed by the assistance of impurities.³⁰ Judging by the doublet structure shown in Fig. 2, the corresponding magnetodonor transitions are allowed for the same reasons. The origin of the assisted transition $2\omega_c + \omega_L$ ($0^+ \rightarrow 2'^+$) has been discussed elsewhere.^{28,31}

The simultaneous observation of both the spin-conserving and the spin-flip transitions allowed us to determine separately the mass anisotropy and the g -value anisotropy. It can be directly seen that the spin-flip transition ($0^+ \rightarrow 2^-$) exhibits a larger anisotropy than the spin-conserving ($0^+ \rightarrow 2^+$) one (even though the former occurs at lower magnetic fields), which means that the g -value anisotropy is larger than that of the mass. This

feature is confirmed by the quantitative estimations given below.

Figure 4 shows the measured energies of the free-electron transitions for the two magnetic-field orientations $\mathbf{B} \parallel (111)$ and $\mathbf{B} \parallel (100)$, compared to the theoretical calculations based on the $5L$ model. As input parameters we have used the measured values of $E_0 = -0.2352$ eV, $E_1 = 3.11$ eV, $\Delta_0 = -0.803$ eV, $\Delta_1 = 0.39$ eV, and the calculated value of $\bar{\Delta} = -0.163$ eV.²⁴ The best fit to the data has been achieved with the following values of adjustable parameters: $E_{p0} = 23.43$ eV, $E_{p1} = 4.923$ eV, $E_Q = 13.99$ eV, $C = -0.4$, and $C' = -0.004$. It can be seen that the theory is in excellent agreement with the data. In particular, the fit determines the value of the matrix element Q , which is responsible for the band's anisotropy within the $5L$ model. The above parameters yield the conduction-band-edge values $m_0^* = 0.01365m_0$ and $g_0^* = -50.9$ (cf. the formulas given in Ref. 16). The nonresonant polaron correction $(1 + \alpha/6)$, where $\alpha = 0.02$, has been included in the calculation of the band-edge effective mass. The above values of m_0^* and g_0^* are in very good agreement with those determined by other authors (cf. Ref. 15).

In order to characterize quantitatively the orbital and spin anisotropy of the conduction electrons in InSb, we have calculated (using the above parameters) the cyclotron masses, defined as $\epsilon_{n+1}^{\pm} - \epsilon_n^{\pm} = \hbar e B / m^*$ and the g values, defined as $\epsilon_{n+1}^+ - \epsilon_n^- = \mu_B g^* B$, for $\mathbf{B} \parallel [001]$ and $\mathbf{B} \parallel [111]$ at $B = 90$ kG. The results are presented in Table I. It can be seen that the anisotropy of the g value is considerably larger than that of the mass for comparable electron energies.

The anisotropies of m^* and g^* are such that both the orbital and spin splittings for $\mathbf{B} \parallel [111]$ are larger than those for $\mathbf{B} \parallel [001]$. The absolute values of $m^*(B)$ and $g^*(B)$ at high fields are considerably different from their

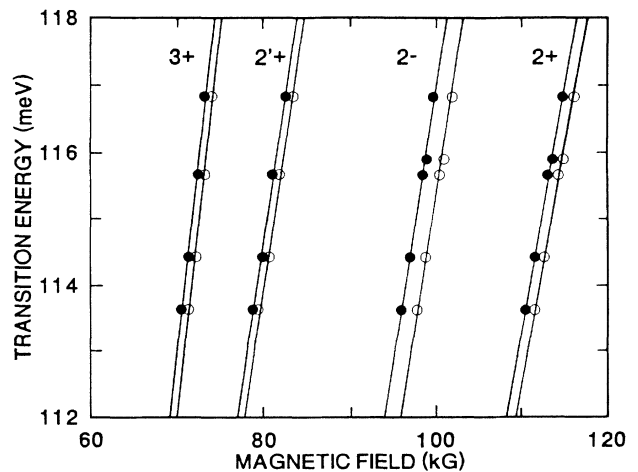


FIG. 4. Energies of the free electron magneto-optical transitions versus magnetic field for the two differently oriented samples studied. The open circles represent the $\mathbf{B} \parallel [111]$ data and the solid circles the $\mathbf{B} \parallel [100]$ data. The solid lines are calculated using the $5L$ $\mathbf{k}\cdot\mathbf{p}$ model.

TABLE I. Effective-mass values and their anisotropy for three CR spin-up (first entry) and spin-down (second entry) transitions in InSb, as calculated for $B=90$ kG with the use of the $5L$ $\mathbf{k}\cdot\mathbf{p}$ model. The effective g values and their anisotropy for the first three Landau levels, as calculated for $B=90$ kG with the use of the same theory (third entry).

CR transition	$\frac{m^*}{m_0}$ [001]	$\frac{m_{001}^*}{m_{111}^*}$
Spin up		
$0^+ \rightarrow 1^+$	0.018 84	0.9955
$1^+ \rightarrow 2^+$	0.024 21	0.9875
$2^+ \rightarrow 3^+$	0.028 53	0.9811
Spin down		
$0^- \rightarrow 1^-$	0.021 22	0.9897
$1^- \rightarrow 2^-$	0.026 08	0.9866
$2^- \rightarrow 3^-$	0.030 16	0.9843
Landau level	g^* [001]	$\frac{g^*_{001}}{g^*_{111}}$
0	-38.05	1.0185
1	-26.16	1.0471
2	-20.25	1.0617

band-edge values, due to the band's strong nonparabolicity. The anisotropy of the conduction band disappears as the energies approach the Γ_6^c band edge. It should also be emphasized that the experimentally confirmed different anisotropies of m^* and g^* follow automatically from the $5L$ model, although the theory uses only one anisotropy matrix element Q .

Concerning the results of other authors, the Ogg²⁰ theory predicted the anisotropy of the g value for the same field directions to be 3.7% for $n=0$, and 11% for $n=1$ (at $B=90$ kG), while Pidgeon, Mitchell, and Brown³² predicted 3.2% for $n=0$ and 7% for $n=1$. These predictions depend, clearly, on the parameters used. It can be seen from Table I that the anisotropy we measure and calculate is somewhat smaller. McCombe⁵ determined experimentally the g -factor anisotropy to be $3.5\% \pm 1.4\%$ for $n=0$, and $10.4\% \pm 4.4\%$ for $n=1$ at $B=90$ kG. Our results agree roughly with the lower bounds for these estimations. It is somewhat difficult to compare directly our experimental results with the spin-resonance data of Chen *et al.*⁶ (cf. also Cardona, Ref. 33) since the two experiments do not involve the same transitions and our excitation energies are about 10 times larger than theirs. However, using our band parameters we also describe very well the g -value anisotropy determined by Chen, Dobrowolska, and Furdyna (Ref. 6, Fig. 4). This means that our anisotropy data agree with and generalize those of Ref. 6.

B. Donor electrons

As we have already mentioned in the experimental section, in addition to the free-electron transitions, magneto-donor (MD) transitions were also observed. In fact, the phonon assistance breaks the selection rules, allowing one

to observe transitions to very high MD states (cf. Littler *et al.*, Ref. 34). Since the calculations of the MD energies in InSb have been presented elsewhere (cf. Zawadzki *et al.*, Ref. 28; also Ref. 35), we will give here only a qualitative description of our procedure.

The important parameter in the theory of MD states is $\gamma = \hbar\omega_c / 2 Ry^*$, characterizing the relative strengths of the magnetic and Coulomb interactions. In InSb, with its small effective mass and high dielectric constant ($\kappa \sim 17$), the effective Rydberg $Ry^* \approx 0.65$ meV is very small. Consequently, at magnetic fields $B > 50$ kG, the value of $\gamma > 30$. In this range of γ values one can calculate the MD energies using the variational procedure with one-parameter trial functions of the magnetic type (cf. Wallis and Bowlden, Ref. 36). The MD functions are described by the three quantum numbers $NM\beta$, in which $N=0, 1, 2, \dots$ and $M=-2, -1, 0, 1, 2, \dots$ characterize the motion transverse to \mathbf{B} , while β characterizes the motion parallel to \mathbf{B} . For $\gamma \gg 1$ a MD state described by $NM\beta$ "belongs" to the Landau subband $n = N + (M + |M|)/2$, its energy being somewhat lower than that of the n th Landau level. Thus, at high magnetic fields one deals with "ladders" of MD states "attached" to each Landau subband.

The variational procedure for the MD energies has been generalized to the case of a nonparabolic band, as described by the $3L$ model.³⁷ However, it would be very tedious to carry out a similar calculation in the framework of the $5L$ model. For this reason, in order to determine the absolute values of the MD energies in the nonparabolic and nonspherical conduction band of InSb, we used the following simpler procedure. We calculate the absolute MD energies using the $3L$ model (nonparabolic but spherical). Then we calculate the free Landau energies in the same $3L$ model. This allows us to calculate the binding energies of the MD states, i.e., the differences between the Landau energy for the n th subband and the corresponding energies of the "attached" MD states. These binding energies are finally subtracted from the Landau energies, as calculated from the $5L$ model. In addition, a detailed analysis shows (cf. Ref. 28) that the variational calculations are particularly simple for the $(0m0)$ states, where $m = |M|$. Moreover, the energies of the $(0m0)$ states are very close to the energies of the respective MD ground states (i.e., attached to the same Landau level $n=m$). Consequently, we calculate the energies of the $(0m0)$ states, identifying them with those of the respective ground states. All MD magneto-optical transitions at low temperatures originate from the lowest ground state (000) .

Figure 5 shows calculated binding energies of the MD states of interest, using the value $Ry^* = 0.65$ meV. In Fig. 6 we show the absolute MD transition energies, calculated using the free-electron energies of Fig. 4 and the binding MD energies of Fig. 5. It can be seen that the calculated MD transition energies are in excellent agreement with the observed transition energies. Since the MD binding energies shown in Fig. 5 are calculated in the spherical model, the good agreement between the experiment and theory for both the free and donor electrons indicates that the anisotropy in the two cases is the

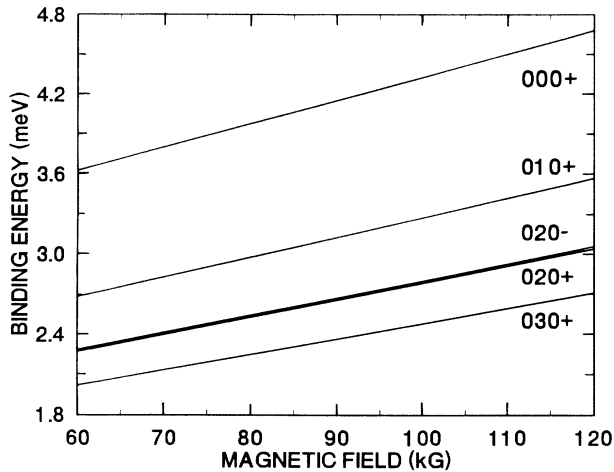


FIG. 5. Binding energies of the magnetodonor states versus magnetic field, as calculated variationally using the $3L$ $\mathbf{k}\cdot\mathbf{p}$ model (cf. Ref. 28).

same. This agrees with and generalizes the result of Bar-ticevitz *et al.*,³⁸ who found that the anisotropy of the g value for the $n=0$ donor electrons in InSb is the same as the g -value anisotropy for the $n=0$ free electrons.

V. SUMMARY

We have investigated, both experimentally and theoretically, the anisotropy of the conduction band of InSb, both in its orbital and spin aspects. Spin-conserving, spin-flip, and phonon-assisted intraband magneto-optical transitions have been observed and successfully described by a five-level $\mathbf{k}\cdot\mathbf{p}$ model, thereby determining the inter-band matrix element Q responsible for the band's anisotropy.

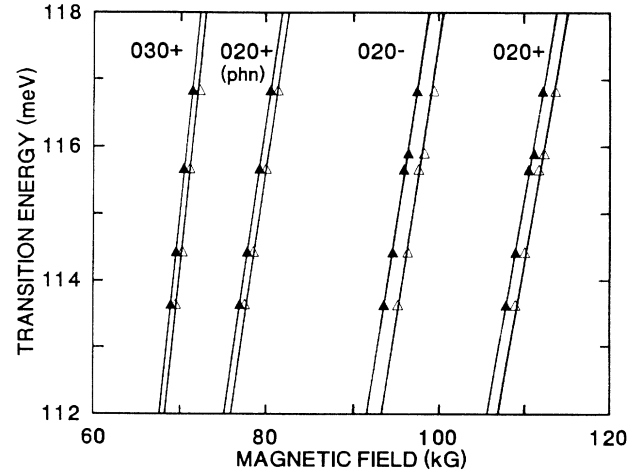


FIG. 6. Energies of the magnetodonor transitions versus magnetic field for the two differently oriented InSb samples. The open triangles represent the $\mathbf{B}\parallel\langle 111 \rangle$ data and the solid triangles the $\mathbf{B}\parallel\langle 100 \rangle$ data. The solid lines are calculated using the $5L$ $\mathbf{k}\cdot\mathbf{p}$ model for the free electrons (cf. Fig. 4) and the magnetodonor theory (cf. Fig. 5).

It has been found that the g -value anisotropy is considerably larger than the mass anisotropy for comparable electron energies. Our g -value results agree with previous estimates of the g -value anisotropy, generalizing them to much higher electron energies. It has also been found that the orbital and spin anisotropies of electrons bound to shallow magnetodonors are the same as those of the free-electron energies.

ACKNOWLEDGMENT

This work was supported in part by National Science Foundation Grant No. DMR-86-17823.

*Permanent address: Institute of Physics, Polish Academy of Sciences, 02-668 Warsaw, Poland.

¹E. O. Kane, *J. Phys. Chem. Solids* **1**, 249 (1957).

²W. Zawadzki, *Adv. Phys.* **23**, 435 (1974).

³G. A. Antcliffe and R. A. Stradling, *Phys. Lett.* **20**, 119 (1966).

⁴D. G. Seiler, *Phys. Lett.* **A31**, 309 (1970).

⁵B. D. McCombe, *Solid State Commun.* **6**, 533 (1968).

⁶Y. F. Chen, M. Dobrowolska, and J. K. Furdyna, *Phys. Rev. B* **31**, 7989 (1985).

⁷R. Bowers and Y. Yafet, *Phys. Rev.* **115**, 1165 (1959).

⁸W. Zawadzki, *Phys. Lett.* **4**, 190 (1963).

⁹E. J. Johnson and D. H. Dickey, *Phys. Rev. B* **1**, 2676 (1970).

¹⁰J. M. Luttinger, *Phys. Rev.* **102**, 1030 (1956).

¹¹C. R. Pidgeon and R. N. Brown, *Phys. Rev.* **146**, 575 (1966).

¹²W. Zawadzki, in *Landau Level Spectroscopy*, edited by G. Landwehr and E. I. Rashba (Elsevier, Amsterdam, 1991), p. 483.

¹³R. Grisar, H. Wachernig, G. Bauer, J. Wlasak, J. Kowalski, and W. Zawadzki, *Phys. Rev. B* **18**, 4355 (1978).

¹⁴M. H. Weiler, R. L. Aggarwal, and B. Lax, *Phys. Rev. B* **17**, 3269 (1978).

¹⁵C. L. Littler, D. G. Seiler, R. Kaplan, and R. J. Wagner,

Phys. Rev. B **27**, 7473 (1983).

¹⁶P. Pfeffer and W. Zawadzki, *Phys. Rev. B* **41**, 1561 (1990).

¹⁷W. Zawadzki, P. Pfeffer, and H. Sigg, *Solid State Commun.* **53**, 777 (1985).

¹⁸H. Sigg, J. A. A. J. Perenboom, P. Pfeffer, and W. Zawadzki, *Solid State Commun.* **61**, 685 (1987).

¹⁹M. A. Hopkins, R. J. Nicholas, P. Pfeffer, W. Zawadzki, D. Gauthier, J. C. Portal, and M. A. DiForte-Poisson, *Semicond. Sci. Technol.* **2**, 568 (1987).

²⁰R. N. Ogg, *Proc. Phys. Soc. London* **89**, 43 (1966).

²¹H. Mayer and U. Rössler, *Phys. Rev. B* **44**, 9048 (1991).

²²Preliminary results of this work have been reported in C. L. Littler, I. T. Yoon, X. N. Song, W. Zawadzki, P. Pfeffer, and D. G. Seiler, in *20th International Conference on the Physics of Semiconductors*, edited by E. M. Anastassakis and J. D. Joannopoulos (World Scientific, Singapore, 1990), p. 1763.

²³V. Evtuhov, *Phys. Rev.* **125**, 1869 (1962).

²⁴I. Gorczyca, P. Pfeffer, and W. Zawadzki, *Semicond. Sci. Technol.* **6**, 963 (1991).

²⁵A. Mycielski, J. Kossut, M. Dobrowolska, and W. Dobrowolski, *J. Phys. C* **15**, 3292 (1982).

²⁶C. Weisbuch and C. Hermann, *Phys. Rev. B* **15**, 816 (1977).

- ²⁷H. Kahlert and D. G. Seiler, *Rev. Sci. Instrum.* **48**, 1017 (1977).
- ²⁸W. Zawadzki, X. N. Song, C. L. Littler, and D. G. Seiler, *Phys. Rev. B* **42**, 5260 (1990).
- ²⁹G. Favrot, R. L. Aggarwal, and B. Lax, *Solid State Commun.* **18**, 577 (1976).
- ³⁰W. Zawadzki, in *Narrow Gap Semiconductors: Physics and Applications*, Lecture Notes in Physics Vol. 133, edited by W. Zawadzki (Springer, Berlin, 1980), p. 85.
- ³¹F. G. Bass and I. B. Levinson, *Zh. Eksp. Teor. Fiz.* **69**, 916 (1965) [*Sov. Phys. JETP* **22**, 635 (1966)].
- ³²C. R. Pidgeon, D. L. Mitchell, and R. N. Brown, *Phys. Rev.* **154**, 737 (1967).
- ³³M. Cardona, *Phys. Rev. B* **34**, 7402 (1986).
- ³⁴C. L. Littler, W. Zawadzki, M. R. Loloee, X. N. Song, and D. G. Seiler, *Phys. Rev. Lett.* **63**, 2845 (1989).
- ³⁵W. Zawadzki, in *Landau Level Spectroscopy*, edited by G. Landwehr and E. I. Rashba (Elsevier, Amsterdam, 1991), p. 1305.
- ³⁶R. F. Wallis and H. J. Bowlden, *Phys. Chem. Solids* **7**, 78 (1958).
- ³⁷W. Zawadzki and J. Wlasak, in *Theoretical Aspects and New Developments in Magneto-Optics*, edited by J. T. Devreese (Plenum, New York, 1980), p. 347. The formulas for the trial energy averages in this paper contain typographical errors (cf. Ref. 28).